

Electrically Driven Flow near a Colloidal Particle Close to an Electrode with a Faradaic Current

W. D. Ristenpart,[†] I. A. Aksay, and D. A. Saville*

Department of Chemical Engineering, Princeton University, Princeton, New Jersey 08544

Received September 30, 2006. In Final Form: December 5, 2006

To elucidate the nature of processes involved in electrically driven particle aggregation in steady fields, flows near a charged spherical colloidal particle next to an electrode were studied. Electrical body forces in diffuse layers near the electrode and the particle surface drive an axisymmetric flow with two components. One is electroosmotic flow (EOF) driven by the action of the applied field on the equilibrium diffuse charge layer near the particle. The other is electrohydrodynamic (EHD) flow arising from the action of the applied field on charge induced in the electrode polarization layer. The EOF component is proportional to the current density and the particle surface (zeta) potential, whereas our scaling analysis shows that the EHD component scales as the product of the current density and applied potential. Under certain conditions, both flows are directed toward the particle, and a superposition of flows from two nearby particles provides a mechanism for aggregation. Analytical calculations of the two flow fields in the limits of infinitesimal double layers and slowly varying current indicate that the EOF and EHD flow are of comparable magnitude near the particle whereas in the far field the EHD flow along the electrode is predominant. Moreover, the dependence of EHD flow on the applied potential provides a possible explanation for the increased variability in aggregation velocities observed at higher field strengths.

Introduction

Situations in which electric fields induce fluid motion are useful in a range of applications. Capillary electrophoresis¹ and the separation of biological macromolecules² are examples of processes where electrokinetics are in play. Emerging applications in microfluidics employ electrokinetic flows for pumping and mixing³ and also to manipulate micrometer-scale objects.⁴ An example of electrically induced flows with striking consequences involves the formation of planar crystalline aggregates, from particles initially widely dispersed across an electrode, in either steady or oscillatory fields.^{5,6} Given the presence of Coulombic and induced-dipole repulsion, aggregation is unexpected. Nevertheless, particles migrate over extended distances (5–10 particle radii) to create large planar structures that break up when the field is removed. The assembly of particles with electric fields is an example of guided self-assembly, a topic of considerable technological potential.⁷ For example, the self-assembly of photonic band gap materials⁸ might benefit from electrokinetic flows. The electric-field patterning of colloids coated with specific biological or catalytic molecules can facilitate the assembly of biosensors⁹ and lab-on-a-chip devices.^{10,11}

The experimental evidence has pointed to electroosmotic flow (EOF) as the primary mechanism of aggregation in steady

fields.^{6,12–14} EOF arises from the action of the steady field on the equilibrium diffuse layers around the particles; therefore, its strength is proportional to the applied field (i.e., the current density) and the particle surface potential. Flows of this sort reverse in concert with the applied field and disappear at frequencies above a few hundred Hertz. Anderson and co-workers measured the approach velocity of particle pairs in steady fields and found a linear dependence on the field strength.^{13,14} Reversal of the field polarity causes aggregates to disperse, indicative of a flow directed away from individual particles.^{6,12–14} Both the linear field strength dependence and sensitivity to polarity are consistent with EOF.¹⁴

Nonetheless, Solomentsev et al.¹⁴ found systematic deviations from the EOF model, especially at higher field strengths. Specifically, they found that both the mean and the standard deviation (i.e., the scatter) of the particle aggregation velocity increased with field strength. They concluded that Brownian motion and EOF were insufficient to explain the deviations, and they hypothesized that the EHD flow proposed by Trau et al.^{5,15} might be involved in the process.

EHD flow involves distortions of the electric field due to the presence of particles that alter the body force distribution in the electrode charge polarization layer.^{5,15} The action of the applied field on this charge produces flow, and because the induced charge and the electrical body force are each proportional to the applied voltage, the flow direction is independent of the field polarity. Nearby particles are mutually entrained and carried toward one another. Because the flow is independent of the polarity, Trau et al. noted that EHD flow is operative in both steady and oscillatory fields. EHD aggregation in ac fields without faradaic currents has been studied by Ristenpart et al. where kinetic experiments¹⁶ and particle-tracking experiments¹⁷ support the EHD mechanism. Aggregation in low-frequency oscillatory

* Corresponding author. (D.A.S.) E-mail: dsaville@princeton.edu. Phone: (609) 258-4585. (D.A.S.) Deceased on October 4, 2006. Direct correspondence to (I.A.A.) E-mail: iaksay@princeton.edu. Phone: (609) 258-4393.

[†] Current address: Division of Engineering and Applied Sciences, Harvard University, Cambridge, Massachusetts 02138.

(1) Russel, W. B.; Saville, D. A.; Schowalter, W. R. *Colloidal Dispersions*; Cambridge University Press: Cambridge, U.K., 1991.

(2) Dai, J. H.; Ito, T.; Sun, L.; Crooks, R. M. *J. Am. Chem. Soc.* **2003**, *125*, 13026–13027.

(3) Squires, T. M.; Bazant, M. Z. *J. Fluid Mech.* **2004**, *509*, 217–252.

(4) Bhatt, K. H.; Grego, S.; Velev, O. D. *Langmuir* **2005**, *21*, 6603–6612.

(5) Trau, M.; Saville, D. A.; Aksay, I. A. *Science* **1996**, *272*, 706–709.

(6) Bohmer, M. *Langmuir* **1996**, *12*, 5747–5750.

(7) Whitesides, G. M.; Grzybowski, B. *Science* **2002**, *295*, 2418–2421.

(8) Joannopoulos, J. D. *Nature* **2001**, *414*, 257–258.

(9) Velev, O. D.; Kaler, E. W. *Langmuir* **1999**, *15*, 3693–3698.

(10) Gau, H.; Herminghaus, S.; Lenz, P.; Lipowsky, R. *Science* **1999**, *283*, 46–49.

(11) Stone, H. A.; Stroock, A. D.; Ajdari, A. *Ann. Rev. Fluid Mech.* **2004**, *36*, 381–411.

(12) Solomentsev, Y.; Bohmer, M.; Anderson, J. L. *Langmuir* **1997**, *13*, 6058–6068.

(13) Guelcher, S. A.; Solomentsev, Y.; Anderson, J. L. *Powder Technol.* **2000**, *110*, 90–97.

(14) Solomentsev, Y.; Guelcher, S. A.; Bevan, M.; Anderson, J. L. *Langmuir* **2000**, *16*, 9208–9216.

(15) Trau, M.; Saville, D. A.; Aksay, I. A. *Langmuir* **1997**, *13*, 6375–6381.

faradaic currents has also been studied by Sides and co-workers,^{18–20} but no work has investigated EHD flow around particles in steady fields.

The aim of our work is to assess the character of electrically driven flows generated in steady fields. The EHD framework originally proposed by Trau et al. is expanded in two contexts. First, a scaling analysis is performed on the basis of a point dipole near an electrode. The key result here is that, contrary to earlier expectations, the EHD velocity scales linearly with the product of the current density and the applied potential (i.e., $u \approx I_f \cdot \Delta\phi$). This scaling result has tremendous implications for experimental interpretation because under typical conditions the current density and applied potential cannot simultaneously be held constant with respect to time. Consequently, measurements in the same cell at different times may yield different results, depending on how significantly the applied potential (or current density) has drifted with time. Moreover, for many electrochemical reactions the current scales exponentially with the applied potential. The resulting logarithmic correction to the field strength dependence obscures the nonlinear behavior and complicates experimental interpretation.

The scaling analysis does confirm, however, that the direction of the EHD flow is independent of the applied polarity because the signs of the applied potential and current density are coupled. The experimental observations, however, demonstrate a polarity dependence. In the second part of the analysis, we investigate whether EHD flow agrees with these observations by calculating the electric potential and resulting EHD streamlines around an individual particle in the limit of thin double layers. The calculations indicate that in the far field the attractive EHD flow is predominant whereas near the particle the flow fields are comparable in magnitude. Surprisingly, the EHD flow very close to the particle is repulsive, but the magnitude of the attractive EOF component is slightly larger, leading to aggregation. These results agree with the observed polarity dependence and provide an explanation for the systematic deviations from the EOF theory observed by Solomentsev et al.¹⁴

The article is organized as follows. First, the potential between parallel electrodes is studied in the context of the (linearized) standard electrokinetic model with a faradaic current. Rather than restricting the treatment to a specific voltage–current relationship, we consider the current density at the electrode to be an independent parameter to focus on the effect of the electrochemical current on the field strength and charge density. Next, a scale analysis of the EHD flow due to a point dipole near the electrode shows that the EHD velocity scales as the product of the bulk field strength and the applied potential whereas EOF is proportional to the field strength. These scaling results inform a more detailed analysis in which an analytical solution depicting the combined effects of EOF and EHD in the thin double layer is derived and streamlines are computed. Under typical conditions, the flow is directed inward toward a test particle and decays as r^{-4} . Comparison with the EOF generated by the particle shows that EHD flow predominates far from the particle whereas close to the particle the EOF and EHD flow are comparable. The theory is then compared to the experimental observations by Solomentsev et al.¹⁴ Specifically, the theory shows that EHD flow contributes significantly to the aggregation and the observed

polarity dependence, and we demonstrate that variations in the applied potential with time could account for the large amount of variability observed in aggregation velocities. The article concludes with a summary of the theoretical results and recommendations for future experimental work.

Electric Potential between Parallel Electrodes

Electrokinetic Model. The theory is based on the standard electrokinetic model as set out by Russel et al.¹ Fluid motion is described by the Stokes equations for low Reynolds number flows with an additional body force due to the presence of free charge. Ion motion is a combination of diffusion, electromigration, and convection whereas electrostatic potential and charge are related by Gauss' equation. Here we focus on 1–1 electrolytes with ions of equal mobilities, and the field equations are

$$0 = -\nabla P - e\left(\sum_i \nu_i n_i\right)\mathbf{E} + \mu\nabla^2\mathbf{u} \quad (1)$$

$$\nabla \cdot \mathbf{u} = 0 \quad (2)$$

$$\frac{\partial n_i}{\partial t} = D_i \nabla^2 n_i \pm e \frac{D_i}{k_B T} \nabla \cdot (n_i \nabla \phi) - \mathbf{u} \cdot \nabla n_i \quad (3)$$

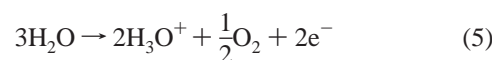
$$-\epsilon\epsilon_0 \nabla^2 \phi = \rho^{(f)} = e \sum_i \nu_i n_i \quad (4)$$

The symbols have their usual meanings: P , pressure; e , charge on a proton; n_i , number density of ions with valence ν_i ; E , electric field strength; μ , viscosity; \mathbf{u} , velocity; D_i , ion diffusivity; $k_B T$, the product of Boltzmann's constant and the absolute temperature; ϕ , electric potential; ϵ , dielectric constant of the liquid; and ϵ_0 , permittivity of free space.

Equation 1 represents the usual momentum balance in the limit of negligible inertia, with an electric body force term. The number densities of ions are related to the electric field through Gauss' equation (eq 4) and also by the conservation relation expressed in eq 3. Here we have employed the Nernst–Planck equation to express the flux of ions; the three terms on the right-hand side of eq 3 represent diffusion, electromigration, and convection, respectively.

This is essentially the model studied by O'Brien and White²¹ and DeLacey and White²² for isolated spheres and the model studied by Ristenpart et al.¹⁷ for particles near electrodes in oscillatory fields. We use the model in the steady-field situation (with a faradaic flux), first between parallel electrodes and then around a particle near an electrode.

“Steady” Fields. Consider two parallel electrodes, separated by a distance $2H$, with the centerline at $z = 0$ and a steady potential $\phi = \Delta\phi$ applied on the electrode at $z = -H$ while the other is grounded. The velocity is zero everywhere, and osmotic pressure balances the electrostatic body force. The flux of ions at each electrode depends on the nature of the electrochemical reactions. For example, in the aqueous systems that have been the main focus of experimental work on particle–particle aggregation, an important electrochemical reaction is the electrolysis of water. Under acidic conditions, this reaction is



(16) Ristenpart, W. D.; Aksay, I. A.; Saville, D. A. *Phys. Rev. E* **2004**, *69*, 021405.

(17) Ristenpart, W. D.; Aksay, I. A.; Saville, D. A. *J. Fluid Mech.* **2007**, *575*, 83–109.

(18) Sides, P. J. *Langmuir* **2001**, *17*, 5791–5800.

(19) Kim, J.; Anderson, J. L.; Garoff, S.; Sides, P. J. *Langmuir* **2002**, *18*, 5387–5391.

(20) Fagan, J. A.; Sides, P. J.; Prieve, D. C. *Langmuir* **2006**, *22*, 9846.

(21) O'Brien, R. W.; White, L. R. *J. Chem. Soc., Faraday Trans. 2* **1978**, *74*, 1607–1626.

(22) Delacey, E. H. B.; White, L. R. *J. Chem. Soc., Faraday Trans. 2* **1981**, *77*, 2007–2039.

at the anode and



at the cathode. The net reaction is $2\text{H}_2\text{O} \rightarrow 2\text{H}_2 + \text{O}_2$. For small applied potentials, the gaseous products readily dissolve in the solution. Typically, a threshold potential must be exceeded before significant current flows; for electrolysis, this value is approximately -1.3 V (SCE). Ionic conduction occurs through the electromigration of hydronium ions, but the concentration of other ionic species (e.g., KCl) is typically larger than that of hydronium ions. The minimum description of charged species in the system requires three ionic concentrations. Denoting species 1 as the cationic ion involved in the electrochemical reaction, the flux is

$$I_f = ej_1 = -eD_1 \frac{dn_1}{dz} - \frac{e^2 D_1 n_1}{k_B T} \frac{d\phi}{dz} \quad (7)$$

where I_f is the current resulting from the faradaic reactions at the electrodes. The fluxes of the other ionic species, which are neither consumed nor produced at the electrodes, vanish:

$$j_2 = 0 = -D_2 \frac{dn_2}{dz} - \frac{eD_2 n_2}{k_B T} \frac{d\phi}{dz} \quad (8)$$

$$j_3 = 0 = -D_3 \frac{dn_3}{dz} + \frac{eD_3 n_3}{k_B T} \frac{d\phi}{dz} \quad (9)$$

The current density I_f depends on a number of factors, including the applied potential, the type of electrodes, and the ionic concentrations.²³ An assumption often made in theoretical analyses is that the current is linearly proportional to the applied potential,^{18,24} although many systems exhibit a current that varies exponentially with the potential, as characterized by the Tafel expression.²³ Rather than restricting our analysis to any specific kinetic model, we first treat the current as an independent parameter to determine its effect on the distributions of charge and potential. This presents no difficulty to the experimentalist because both the current density and potential difference are readily measured simultaneously. We emphasize that the current density is not independent of the applied potential; moreover, the range of possible values for I_f is constrained by the sign of the applied potential and the limiting current.²³ Nonetheless, we leave the details of the electrochemistry unspecified to focus on the resulting hydrodynamics.

Some caution, however, is required with regard to the transient nature of the current. Although the term “steady” is widely used to denote a situation where the electric field is invariant in time, care must be taken to specify what is invariant. In electrochemical cells, there are two types of steady systems: potentiostatic and galvanostatic. In potentiostatic systems, the potential difference between the electrodes is held constant, and the current is allowed to vary with time. In galvanostatic systems, the potential difference is continuously adjusted so as to maintain a constant current across the cell. Because the electric field strength in the bulk of the cell is proportional to the current density, most investigators employ galvanostatic techniques to obtain a steady field in the bulk, but this neglects the changing potential difference at the electrode surfaces where EHD effects are produced. It is important to note that neither potentiostatic nor galvanostatic systems are

truly steady because the current density or potential difference changes with time. As we shall see, however, when the rate of change is slow enough we can treat the system as pseudosteady. For the sake of brevity, we focus on the galvanostatic case and simply note that a similar analysis applies for the potentiostatic case.

It is well known that a suddenly applied potential yields a current that decays with time as a result of concentration polarization at the electrode. Likewise, a suddenly imposed current requires an applied potential that increases with time. For example, in diffusion-limited systems near a planar electrode the Cottrell equation, $I_f = Kt^{-1/2}$, is often used to describe the temporal decay after application of a potential; the prefactor K is a function of the ionic diffusivities and initial concentration.²³ However, this expression neglects electromigration and convection and is not applicable in the general case of interest here. Absent more specific information, we turn to dimensional analysis to identify appropriate restrictions. Time dependence enters the electrokinetic model explicitly only via ion conservation (cf. eq 3). Specifying scaling parameters for length (H), potential ($e/k_B T$), and concentration (n_∞) yields

$$\frac{H^2}{t^* D} \frac{\partial \hat{n}_i}{\partial \hat{t}} = \nabla^2 \hat{n}_i \pm \nabla \cdot (\hat{n}_i \nabla \hat{\phi}) \quad (10)$$

where t^* is a characteristic time. Clearly the system may be treated as pseudosteady provided

$$t^* \gg \frac{H^2}{D} \quad (11)$$

For hydronium ions in a $100 \mu\text{m}$ cell, H^2/D is approximately 1 s, so when the current density changes on a longer time scale, the system is pseudosteady.

Defining a dimensionless charge density \hat{n} as

$$\hat{n} \equiv \frac{n_1^\infty}{n_2^\infty} (1 + \hat{n}_1) + \hat{n}_2 - \hat{n}_3, \quad (12)$$

where for simplicity we have assumed that $n_\infty = n_2^\infty = n_3^\infty \gg n_1^\infty$, allows the equations describing charge conservation and the electric potential to be solved. The boundary conditions involve the specification of the potential and flux of each species on the electrodes along with a symmetry condition,

$$\hat{n} = 0, \hat{y} = 0 \quad (13)$$

Conservation of charge requires the current flux at each electrode to be identical, preventing the formation of asymmetrical charge distributions in a stationary (steady-state) system.

Linearization and solution yield (in dimensional terms)

$$\phi = \frac{\Delta\phi}{2} \left(1 - \frac{\sinh \kappa z}{\sinh \kappa H} \right) - \frac{I_f H}{\sigma_\infty} \left(z - \frac{\sinh \kappa z}{\sinh \kappa H} \right) \quad (14)$$

$$\rho^{(f)} = \frac{e^2 n_2^\infty}{k_B T} \left(\Delta\phi - \frac{I_f H}{\sigma_\infty} \right) \frac{\sinh \kappa z}{\sinh \kappa H} \quad (15)$$

Here the Debye length is defined as $\kappa^{-1} = (k_B T / 2n_\infty e^2)^{1/2}$ and the bulk conductivity is $\sigma_\infty = 2e^2 D_1 n_2^\infty / k_B T$. Note that the first term in eq 14 is equivalent to the Gouy–Chapman model between parallel plates.¹ For $\kappa H \gg 1$ and absent a faradaic reaction, we see that the potential drop occurs entirely across the polarization layers near the electrodes and the electric field strength in the bulk is zero. If the applied potential exceeds the redox potential,

(23) Newman, J. *Electrochemical Systems*; Prentice Hall: Englewood Cliffs, NJ, 1973.

(24) Fagan, J. A.; Sides, P. J.; Prieve, D. C. *Langmuir* **2004**, *20*, 4823–4834.

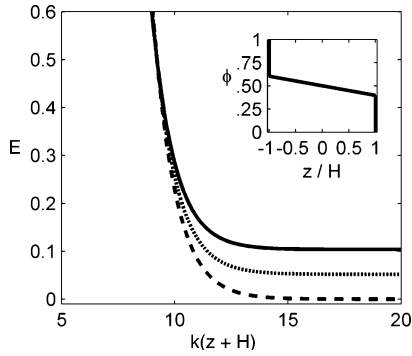


Figure 1. Dimensionless electric field strength between parallel electrodes for a steady applied potential resulting in different faradaic current densities: (---), $I_f = 0$; (···), $I_f = 50 \mu\text{A}/\text{cm}^2$; (—), $I_f = 100 \mu\text{A}/\text{cm}^2$. (Inset) dimensionless potential across the entire cell for $I_f = 100 \mu\text{A}/\text{cm}^2$. Parameters: $\kappa^{-1} = 10 \text{ nm}$, $H = 100 \mu\text{m}$, and $\Delta\phi = 1 \text{ V}$.

then current begins to flow and the field strength well away from the electrodes is nonzero. Representative plots of the field strength for different current densities are depicted in Figure 1. Outside of the polarization layer near the electrodes, the field strength is

$$E = -\frac{d\phi}{dz} \cong \frac{I_f}{\sigma_\infty} \quad z \rightarrow 0 \quad (16)$$

For small current densities, the (area) charge density in the polarization layer near the powered electrode is

$$q = -\epsilon\epsilon_0 \frac{d\phi}{dz} \cong -\frac{\epsilon\epsilon_0 \kappa \Delta\phi}{2} \quad z \rightarrow -H \quad (17)$$

This expression is accurate if the charge contribution due to the current is negligible compared to the charge density arising from polarization, in other words, if the current obeys the inequality

$$I_f \ll \frac{\sigma_\infty \Delta\phi}{2H} \quad (18)$$

which is readily satisfied for typical systems.

Scaling Analysis: EHD Flow near a Point Dipole

To examine the EHD flow arising from a particle adjacent to an electrode, we follow the analysis used for oscillatory fields.¹⁶ The particle perturbs the otherwise uniform field, inducing a force on the charge in the polarization layer and creating flow. The flow mechanism differs from classical electroosmosis in both the origin and dynamics of the charge distribution. In the classical model, the mobile equilibrium charge in the fluid balances charge that is chemically bound to solid–liquid interfaces; here the charge in the fluid is proportional to the externally imposed potential. Because the induced charge is proportional to the applied potential, electrical stresses scale nonlinearly with the field strength, and the response is justifiably designated as an EHD flow.²⁵

The relation between the tangential electrical stresses and velocity is expressed by the Helmholtz–Smoluchowski equation for steady electroosmosis in a diffuse layer along a rigid, charged interface.¹ Within the charge layer, electrical stresses are balanced by viscous shear whereas outside the Debye layer the fluid velocity is asymptotic to the Helmholtz–Smoluchowski value,

$$u^* = \frac{\epsilon\epsilon_0 \Delta\phi}{\mu} E_t \quad (19)$$

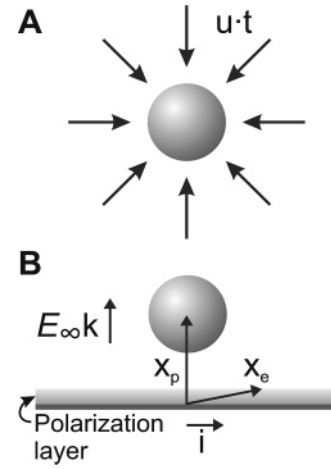


Figure 2. Definition sketch depicting a spherical particle near an electrode. (A) Plan view depicting flow toward the test particle under conditions where the inequality $C_0 < 0$ is satisfied. (B) Elevation view showing a particle located at \mathbf{x}_p outside the polarization layer; \mathbf{x}_e denotes a point in the polarization layer near the electrode, with $\mathbf{x}_e \cdot \mathbf{k} \approx 0$.

Here $\Delta\phi$ is the electrostatic potential at the electrode solid–fluid interface, and E_t is the tangential component of the applied electric field. For a negatively charged surface, $\Delta\phi < 0$, and the action of the field on positively charged counterions produces fluid motion in the direction of the field. It is useful to rewrite this expression using Gauss' law to relate the potential gradient and q , the total charge per unit area in the diffuse layer, as a balance between the electric and viscous stresses on the Debye scale:

$$\mu \frac{u^*}{\kappa^{-1}} = -\frac{\epsilon\epsilon_0 \zeta}{\kappa^{-1}} E_t = qE_t \quad (20)$$

According to eq 20, the induced velocity is proportional to the electrical stress per unit area, qE_t .

As a first approximation for the EHD flow, we neglect particle–electrode interactions and portray the particle's influence in terms of a point-dipole approximation. The electric potential around a particle in the uniform field well outside the diffuse layer is

$$\phi = -aE_\infty \left[(\mathbf{x} - \mathbf{x}_p) \cdot \mathbf{k} - C_0 \frac{(\mathbf{x} - \mathbf{x}_p) \cdot \mathbf{k}}{r^3} \right] \quad (21)$$

Here, $E_\infty = I_f/\sigma$ is the incident field strength, \mathbf{x} and \mathbf{x}_p are vectors (scaled with the particle radius) for the position and the location of the center of the particle (Figure 2), r is the (scaled) distance from the particle center, and C_0 is the dimensionless dipole coefficient. For a dielectric particle in a dielectric medium, the dipole coefficient is a real quantity given by the Clausius–Mossotti formula,²⁶ viz., $(\epsilon_p - \epsilon)/(\epsilon_p + 2\epsilon)$. Because we are dealing with charged particles suspended in an electrolyte, C_0 depends on the properties of the particle (ζ potential or surface charge and radius) and electrolyte (ionic strength, ion valences and mobilities, and dielectric constant). Accordingly, the dipole coefficient is best computed using the zero-frequency limit of the standard electrokinetic model.²¹

At \mathbf{x}_e , a point close to the electrode (near $z = -H$), the x component of the electric field around the point dipole is

$$\mathbf{E} \cdot \mathbf{i} = 3E_\infty C_0 \frac{[(\mathbf{x}_e - \mathbf{x}_p) \cdot \mathbf{k}](\mathbf{x}_e \cdot \mathbf{i})}{r^5} \approx -3E_\infty C_0 \frac{(\mathbf{x}_p \cdot \mathbf{k})(\mathbf{x}_e \cdot \mathbf{i})}{r^5} \quad (22)$$

Combining eqs 16, 17, and 22 with eq 20 gives

$$qE_t \approx 3\epsilon\epsilon_0 \frac{\Delta\phi}{\kappa^{-1}} E_\infty C_0 \frac{(\mathbf{x}_p \cdot \mathbf{k})(\mathbf{x}_e \cdot \mathbf{i})}{r^5} \quad (23)$$

It follows that the tangential velocity due to EHD forces scales with the normal and tangential components of the field as

$$\mathbf{u} \cdot \mathbf{t} \approx \frac{3\epsilon\epsilon_0 \Delta\phi E_\infty C_0}{\mu} f(\mathbf{r}) \quad (24)$$

where $f(\mathbf{r}) \approx r^{-4}$ denotes a dimensionless function related to the position \mathbf{x}_p . As with oscillatory fields,¹⁶ the direction of the fluid flow depends on the sign of the dipole coefficient but is independent of the polarity. If $C_0 < 0$, then flow is directed toward the particle.

Because the electroosmotic velocity due to slip on the particle scales as

$$u_{\text{EOF}} \approx \frac{\epsilon\epsilon_0 \zeta E_\infty}{\mu} \quad (25)$$

where ζ is the particle surface potential, comparison of the EOF and EHD velocities yields the ratio

$$\frac{u_{\text{EOF}}}{u_{\text{EHD}}} \approx \frac{\zeta}{3C_0 \Delta\phi} \quad (26)$$

For particle zeta potentials on the order of 100 mV and $\Delta\phi > 1$ V, this ratio is on the order of 1. The scale analysis suggests that both EOF and EHD flow contribute to the particle aggregation, and a more thorough analysis will be useful.

In regard to experimental verification of the aggregation mechanism, the scale analysis yields two important observations. First, an apparent linear field strength dependence may be insufficient by itself to decide whether EOF or EHD flow is responsible for the observed aggregation. Although EHD flow is nonlinear, because it depends on the product of the applied potential and the bulk field strength, in many situations of interest²⁷ the current density depends exponentially on the applied potential.²⁸ For example, many electrochemical reactions driven at applied potentials much greater than the redox potential are described by the Tafel equation

$$I_f = i_o \exp\left(\frac{\alpha n F (\Delta\phi - \phi_{\text{redox}})}{RT}\right) \quad (27)$$

where α is a reaction symmetry parameter, n is the number of electrons involved in the reaction, and i_o is the equilibrium exchange current density.²³ In this situation, the resulting field strength dependence for EHD flow is linear with a logarithmic correction

$$u_{\text{EHD}} \approx E_\infty \log E_\infty \quad (28)$$

This dependence may be difficult to detect, especially when the flow field is superimposed with a truly linear driving force (EOF).

The second observation is that aggregation induced by faradaic currents cannot be considered to take place under steady conditions

(25) Saville, D. A. *Ann. Rev. Fluid Mech.* **1997**, *29*, 27–64.

(26) Jackson, J. D. *Classical Electrodynamics*, 2nd ed.; John Wiley & Sons: New York, 1975.

(27) Guelcher, S. A. Investigating the Mechanism of Aggregation of Colloidal Particles during Electrophoretic Deposition. Ph.D. Thesis, Carnegie Mellon University, 1999.

(28) In his study of particle aggregation, Guelcher reported that applied potentials of approximately 0.95, 1.39, and 1.45 V on gold electrodes in 0.1 M KClO₄ correspond to current densities of 1.3, 6.5, and 13 $\mu\text{A}/\text{cm}^2$, respectively, an apparent exponential increase (ref 27, chapter 4).

because either the applied potential or current density is necessarily changing with time. Experimentally, this necessitates careful observations of both the potential and current density during aggregation to ensure that the magnitude of EHD flow is consistent between experiments. We return to this issue after examining the more detailed theory, and we hypothesize that variations in the applied potential, and consequently the EHD flow, are responsible for the increased scatter observed at higher field strengths.

Analytical Model and Streamlines

Thin-Double-Layer Model. Obtaining the potential distribution between parallel electrodes is straightforward because there are only two length scales: the Debye length and the electrode separation. When a particle is present, the problem is complicated by two additional length scales: the particle radius and the distance h between the electrode and particle surface. One of the length scales can be removed if we restrict our attention to situations where the particle is small compared to the electrode separation (i.e., $H \gg a$ and $H \gg h$). The domain can then be treated as semi-infinite, with a far-field condition equivalent to the potential distribution in the absence of the particle. In most experiments, the Debye length is much smaller than the particle length scale ($\kappa a \gg 1$), suggesting that the thin-double-layer approximation is applicable. The thin-double-layer limit has been extensively studied in the context of both isolated particles^{29–31} and particles near electrodes.^{32,33}

To capture the effects of electroosmosis near the particle, one needs to take account of the properties of the double layer. In the diffuse part of the double layer near the particle surface, the nonzero charge concentration gives rise to both a higher ionic conductivity and electroosmotic flow. As demonstrated by O'Brien,³⁴ who extended the earlier work of O'Konski³⁵ and Dukhin and Shilov,³⁶ both effects can be captured for thin layers by invoking the concept of a surface conductivity. A current balance applied to a slab-shaped control volume on the particle surface yields the boundary equation

$$\sigma_\infty \nabla\phi \cdot \mathbf{n} - \sigma_p \nabla\phi_p \cdot \mathbf{n} = -\sigma_s \nabla_s^2 \phi \quad r = a \quad (29)$$

where σ_∞ and σ_p are the ionic conductivities of the fluid and particle, respectively, σ_s is the particle surface conductivity, and ∇_s^2 denotes the surface gradient. The terms on the left-hand side of the equation represent the normal current flux into the particle surface, whereas the term on the right-hand side represents the tangential current flux along the particle surface. The surface conductivity σ_s depends on the amount of free charge in the double layer (or equivalently, the surface potential) and can be estimated with the Bikerman equation³⁷

$$\sigma_s = \frac{\sigma_\infty}{\kappa} \left(\exp\left[\frac{e\zeta}{2k_B T}\right] - 1 \right) (1 + 3M_D) \quad (30)$$

Here, ζ is the particle surface potential, and M_D is the dimensionless ionic drag coefficient. To simplify the problem further, we note that for most systems of interest (e.g., polystyrene

(29) O'Brien, R. W.; Ward, D. N. *J. Colloid Interface Sci.* **1988**, *121*, 402–413.

(30) Melcher, J. R.; Taylor, G. I. *Ann. Rev. Fluid Mech.* **1969**, *1*, 111.

(31) Shilov, V. N.; Dukhin, S. S. *Colloid J. USSR* **1970**, *32*, 90.

(32) Morrison, F. A.; Stukel, J. J. *J. Colloid Interface Sci.* **1970**, *33*, 88.

(33) Reed, L. D.; Morrison, F. A. *J. Colloid Interface Sci.* **1976**, *54*, 117–133.

(34) O'Brien, R. W. *J. Colloid Interface Sci.* **1986**, *113*, 81–93.

(35) O'Konski, C. T. *J. Phys. Chem.* **1960**, *64*, 605–619.

(36) Dukhin, S. S.; Shilov, V. N. *Adv. Colloid Interface Sci.* **1980**, *13*, 153–195.

(37) Bikerman, J. J. *Trans. Faraday Soc.* **1939**, *36*, 154–160.

or silica in water) the conductivity of the particle is negligible, so here we specify $\sigma_p = 0$.

With eq 29 established as the appropriate condition for the electric potential on the particle surface, the final ingredient required is the electrode boundary condition. This boundary condition has received relatively little attention in the context of particles near electrodes. Previous workers studying particles near electrodes in the limit of thin double layers have often assumed a constant potential along the electrode,^{12,32} presumably motivated by the equipotential requirement for conducting objects. However, the relevant electrokinetic quantity is not the potential on the electrode surface but rather *the potential and charge within the polarization layer*. Tangential potential gradients arise in the double layer, even when adjacent to an equipotential conductor, and in the limit of thin double layers it is the potential at the “edge” of the polarization layer that governs the electrokinetic response.^{3,38} Flows induced around conducting objects have been extensively studied in the Russian literature; a recent review is provided by Squires and Bazant.³

The challenge is to determine the effect of the particle on the potential distribution at the edge of the polarization layer near the electrode. For steady fields, however, one must specify more about the nature of the electrochemical reaction, which in general depends on the values of the local potential and charge concentrations. To facilitate analytical progress, we restrict our attention to electrochemical reactions that are relatively insensitive to potential fluctuations. Following Newman,²³ a dimensionless number

$$J = \frac{(\alpha_c + \alpha_a) a i_o F}{\sigma_\infty R T} \quad (31)$$

governs the electrochemical response. Here F is Faraday’s constant, α_i represents the kinetic symmetry parameters, i_o is the exchange current density, and R is the gas constant. This expression quantifies the ratio of ohmic resistance (along a distance a) to the charge-transfer resistance of the electrochemical reaction. Large values of J indicate a “fast” reaction such that the resistance to current in the electrolyte is dominant, and small values of J indicate a “slow” reaction where charge-transfer kinetics at the electrode dominate. Thus, for values of $J \ll 1$ the current density tends toward uniformity along the electrode, and with reactions that satisfy this criterion, the electric field strength may be modeled as constant along the electrode,

$$\nabla\phi \cdot \mathbf{n} = -\frac{I_f}{\sigma_\infty} \quad z = 0 \quad (32)$$

Note that for convenience in the semi-infinite domain we redefine the electrode position as $z = 0$. Similar constant-field-strength boundary conditions on the electrode were studied by Ristenpart et al.¹⁷ in the context of high-frequency oscillatory fields without faradaic reactions and by Sides and co-workers for oscillatory faradaic currents at lower frequencies.²⁴

Model Calculations. To recapitulate, the electrostatic model to be solved is

$$\nabla^2\phi = 0 \quad (33)$$

$$\nabla\phi \cdot \mathbf{n} = -E_\infty \quad z = 0 \quad (34)$$

$$\nabla\phi \cdot \mathbf{n} \rightarrow -E_\infty \quad z \rightarrow \infty \quad (35)$$

$$\sigma_\infty \nabla\phi \cdot \mathbf{n} = -\sigma_s \nabla_s^2 \phi \quad r = a \quad (36)$$

The hydrodynamics are modeled as follows. In the thin-double-

layer limit, the EHD body force (cf. eq 1) is identically zero, and flow is governed by solutions to the Stokes equations. Far from the particle, the velocity is expected to decay to zero, and the normal velocity must be zero on all solid surfaces. The tangential velocities on the electrode and particle surface satisfy the electroosmotic velocities. Because of the linearity of the problem, the electrically induced flow can be studied in two parts: (i) EHD flow driven by perturbations of the field and charge near the electrode due to the presence of the particle and (ii) EOF due to the action of the field on the charge in the particle’s diffuse layer. To calculate the EOF generated along the particle, a Smoluchowski velocity (eq 19) is applied on the particle surface, and a no-slip condition is applied on the electrode. To calculate the EHD flow generated along the electrode, a no-slip condition is applied on the particle surface, and a Smoluchowski slip velocity is applied on the electrode. The charge density on the electrode is approximated by eq 17

$$q = -\frac{\epsilon\epsilon_o\kappa\Delta\phi}{2} \quad (37)$$

which is valid if eq 18 is satisfied. We emphasize that this expression for the charge density is an approximation; for the slow reactions studied here ($J \ll 1$), we assume that both the current density and charge density are uniform on the electrode. Accordingly, the model is as follows:

$$\text{In the domain: } -\nabla P + \mu \nabla^2 \mathbf{u} = 0 \quad (38)$$

$$\text{Both surfaces } (z = 0, r = a): \mathbf{u} \cdot \mathbf{n} = 0 \quad (39)$$

$$\text{On the electrode } (z = 0): \mathbf{u} \cdot \mathbf{t} = \begin{cases} 0 & \text{(EOF)} \\ qE/\mu\kappa & \text{(EHD)} \end{cases} \quad (40)$$

$$\text{On the particle } (r = a): \mathbf{u} \cdot \mathbf{t} = \begin{cases} \epsilon\epsilon_o\zeta E/\mu & \text{(EOF)} \\ 0 & \text{(EHD)} \end{cases} \quad (41)$$

To solve these systems of equations, we employ separation of variables in bispherical coordinates, as originally proposed by Morrison and Stukel,³² and use stream functions to represent the flow. The mathematical procedure is identical to the one discussed by Ristenpart et al.^{17,39} for oscillatory fields and will not be reproduced here. Indeed, the shapes of the resulting equipotentials⁴⁰ and streamlines for EHD flow are identical for oscillatory fields and steady fields (Figures 3 and 4), though the magnitudes differ.

Comparison of EOF and EHD Flow. Representative equipotential plots are presented in Figure 3. For a particle with zero surface conductivity, the equipotential lines around a particle adjacent to an electrode are similar to those of an isolated insulating particle, but the presence of the electrode clearly distorts the field (Figure 3A). The condition of constant field strength on the electrode results in a nonuniform potential underneath the particle. For a particle with zero or low surface conductivity, the gradient in potential along the electrode is directed *away* from the particle. The situation is reversed for particles with high surface conductivity (Figure 3B). Here the equipotential lines

(38) Bazant, M. Z.; Squires, T. M. *Phys. Rev. Lett.* **2004**, *92*, 066101.

(39) Ristenpart, W. D. *Electric-Field Induced Assembly of Colloidal Particles*. Ph.D. Thesis, Princeton University, 2005.

(40) Note that the equipotential lines are equivalent for steady fields and for oscillatory fields at time $t = 2\pi n/\omega$, where n is any integer. The magnitude of the potential, however, depends on the value of E_∞ appropriate for a steady or oscillatory field.

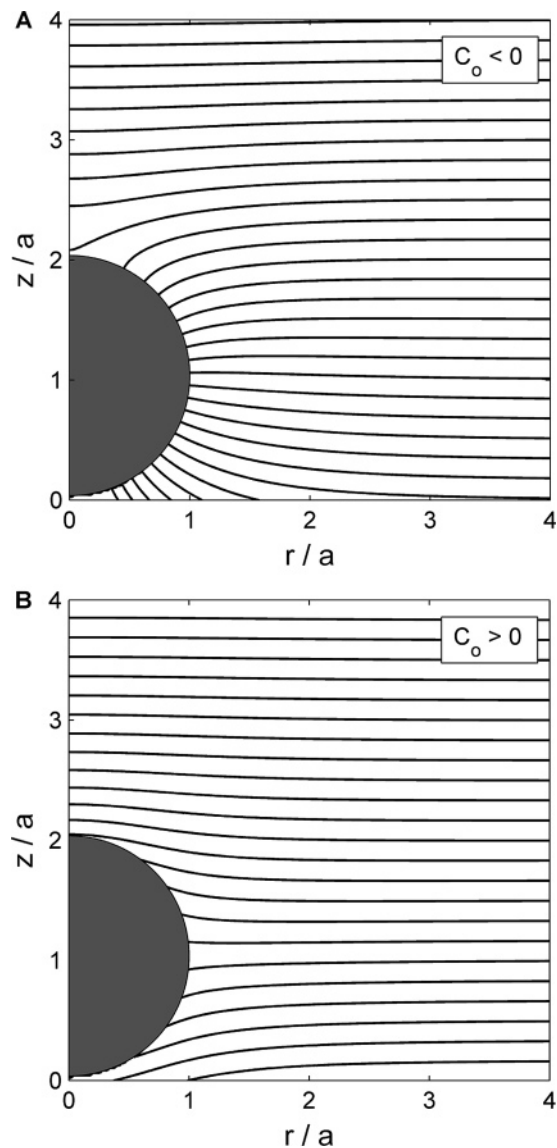


Figure 3. Electric potential around a particle near an electrode subject to a uniform (radially invariant) current density. The particle is located at $z/a = 0.0375$. (A) $\sigma_S = 0$, equivalent dipole strength $C_0 = -0.5$. The gradient in potential along the electrode is directed *away* from the particle. (B) $\sigma_S = 4.5 \times 10^{-4}$ S, equivalent dipole strength $C_0 = +0.25$. The gradient in potential along the electrode is directed *toward* the particle.

are similar to those of an isolated conducting particle, and underneath the particle the potential gradient is directed *toward* the particle.

Representative streamlines due to EOF along the particle are presented in Figure 4A for a particle located at $z/a = 0.0375$. The flow structure is toroidal, with the recirculation centered above the particle ($z/a \approx 2$). The velocity is greatest in magnitude along the vertical edge of the particle. The flow structure is qualitatively similar to that reported by Solomentsev et al.,¹² despite the different boundary conditions employed here (i.e., constant field strength on the electrode rather than constant potential). The direction of the flow depends on the sign of the particle zeta potential and the polarity of the field; for negative zeta potentials and positive fields, the flow moves in the clockwise direction.

The streamlines due to EHD flow generated on the electrode are presented in Figure 4B. Like EOF, the EHD flow is toroidal, but it recirculates about a point located below the particle edge ($z/a \approx 0.5$). The velocity increases rapidly underneath the particle

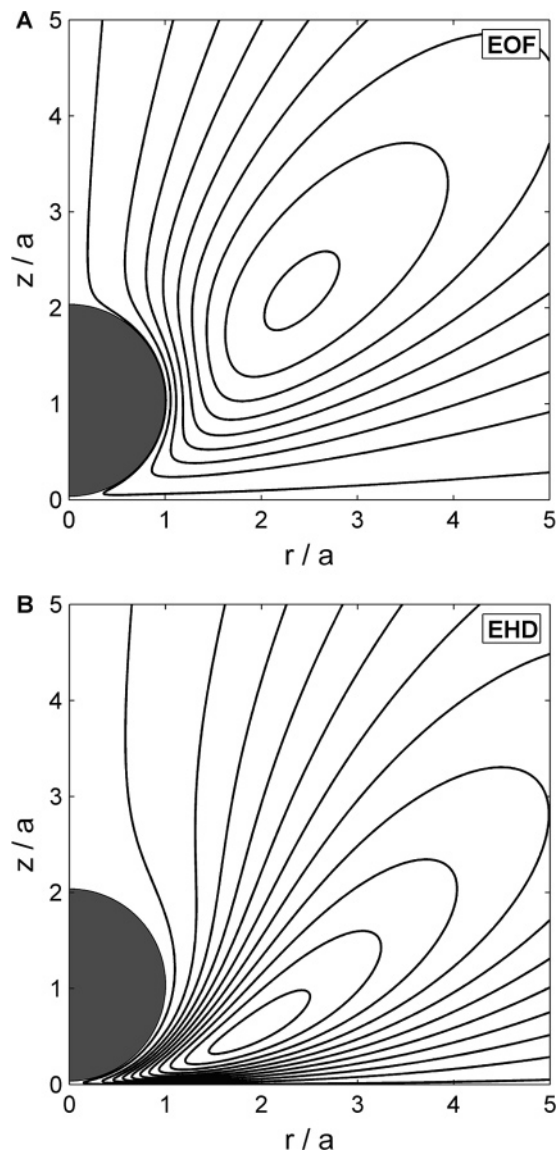


Figure 4. Streamlines for electrically driven flow around a charged spherical colloid near an electrode with a faradaic current. The particle is located at $z/a = 1.04$. (A) Electroosmotic streamlines generated by slip along the particle surface. For anodic currents (electric field oriented in the positive z direction), the direction of flow is clockwise for $\zeta < 0$ and counterclockwise for $\zeta > 0$. (B) EHD flow generated by slip along the electrode. The direction of flow is clockwise for $C_0 < 0$ and counterclockwise for $C_0 > 0$, regardless of the field polarity.

before quickly changing direction and moving away from the particle. Here, the direction of flow is independent of the field polarity and depends only on the dipole coefficient of the particle. For $C_0 < 0$, the flow direction is clockwise.

As with EHD flow in oscillatory fields,¹⁷ the far-field ($r/a \gg 1$) radial component of both EOF and EHD flow in steady fields decays as r^{-4} . The streamlines reveal an important difference in the radially directed component of the flow in the near field, however. In the EOF case, at the particle center line ($z/a = 1.0375$) the flow is directed radially inward for all values of $r/a > 1$. For EHD flow, the radial component changes direction at approximately $r/a = 2.5$; the flow is directed radially inward for $r/a > 2.5$ and radially outward for $r/a < 2.5$. This suggests that EHD flow induces aggregation of widely separated particles but hinders aggregation at close separations. However, the actual effect on a nearby particle also depends on the gradient of the flow field, as discussed in the next section.

Comparison with Experiments

The true flow field around the particle is the superposition of EOF and EHD flow, the magnitudes of which depend on the electric field and particle parameters. Here we focus on the experimental conditions employed by Solomentsev et al.¹⁴ We briefly summarize their results and then demonstrate that, contrary to earlier expectations, EHD flow is consistent with their observations and might explain some unresolved features of their work.

In their experiments, Solomentsev et al. measured the separation distance between 9.7- μm -diameter polystyrene particles ($\zeta = -65$ mV) versus time as they aggregated in a range of electric field strengths (20–100 V/m). The particles were suspended in 1 mM sodium bicarbonate ($\kappa a \approx 500$) over thin-film gold electrodes; their measurements by total internal reflection microscopy indicated that the particles floated an average of 182 nm over the surface of the electrode ($h/a = 0.0375$).

To begin an experiment, Solomentsev et al. found two adjacent particles well separated from any other particles, applied the field, and then measured their separation distance once the particles reached $r/a = 3.5$ until contact. They averaged the trajectories of at least 10 particle pairs for each of several different applied field strengths. Their main conclusions are as follows:

(1) The particle aggregation velocity depends linearly on the applied field strength.

(2) The particle trajectory depends on the field polarity; reversing the polarity induces aggregated particles to separate (consistent with previous observations).^{6,12}

(3) As the electric field strength is increased, the particle trajectories are increasingly scattered (i.e., the standard deviation of the particle position versus time increases); Brownian motion is insufficient to explain the scatter.

Comparison with EHD Theory. As discussed previously, the apparent linear field strength dependence may be difficult to differentiate from a linear dependence with a logarithmic correction. To make further progress, more information about the kinetics of the electrochemical reaction is necessary to determine the expected EHD field strength dependence. Because these details are unavailable, we instead focus our attention on the other two observations. Our calculations demonstrate that both the polarity dependence and increased scatter are consistent with EHD flow.

The streamlines for the combination of EOF and EHD flow are presented in Figure 5A using parameters that are valid for the experimental conditions used by Solomentsev et al.¹⁴ and assuming a positive polarity ($\Delta\phi = 1$ V). The flow structure is clearly affected by both EOF and EHD flow. The flow recirculates around a point located near $z/a = 1.5$, which is intermediate between the centers of recirculation for the individual flow fields (Figure 4). In comparison to pure EOF, more fluid is pulled underneath the particle in the combined flow. Moreover, the radial component of the flow at the particle center line ($z/a = 1.0375$) exhibits a change in the direction of flow near $r/a = 2.2$; the flow is radially inward for $r/a > 2.2$ and radially outward for $r/a < 2.2$.

To calculate the effect of the flow field on a nearby particle, we follow Solomentsev et al.¹⁴ and express the velocity of particle 2 induced by the flow field of particle 1 by using Faxen's law

$$\mathbf{u}_2 \cdot \mathbf{i} = \left(\mathbf{u}_1 + \frac{a^2}{6} \nabla^2 \mathbf{u}_1 \right) \cdot \mathbf{i} \quad (42)$$

where the velocity \mathbf{u}_1 is evaluated at the position occupied by particle 2. Note that Faxen's law strictly applies only to unbounded

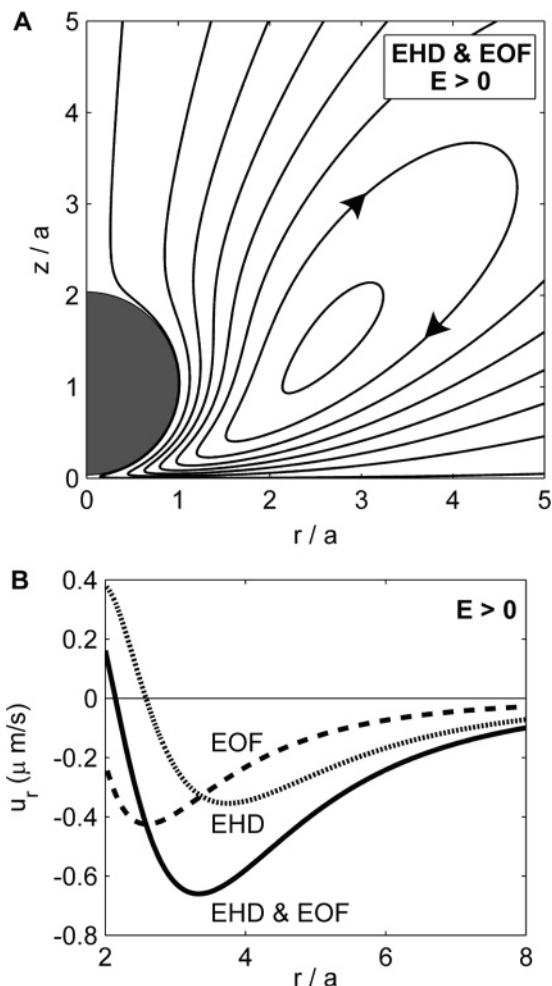


Figure 5. Superposition of EOF and EHD flow for the experimental conditions reported by Solomentsev et al.,¹⁴ assuming a positive polarity and applied potential of $\Delta\phi = 1$ V. Parameters: $a = 4.85$ μm , $h = 182$ nm, $\zeta = -65$ mV, $[\text{NaHCO}_3] = 10^{-3}$ M, and $I_f = 90$ $\mu\text{A}/\text{cm}^2$. (A) Streamlines for the superposition of EOF and EHD flow. Arrows indicate the direction of flow. (B) Radial particle-pair aggregation velocity due to electrically induced flow. Symbols: ($\bullet\bullet$), EHD velocity; ($--$), EOF velocity; ($-$), combined EOF and EHD. Negative values indicate that the flow is directed radially inward toward each particle, inducing aggregation. The combined flow is weakly repulsive at very close separations but strongly attractive at larger distances.

fluids and is thus an approximation.⁴¹ The particle-pair aggregation velocity⁴² is then

$$u_r = 2q(h)(\mathbf{u}_2 \cdot \mathbf{i}) \quad (43)$$

Here q is a wall hindrance coefficient that depends weakly on the particle height; following O'Neill's method,⁴³ Solomentsev et al. found that $q = 0.365$ for their particles. The factor of 2 accounts for the influence of each particle on the other.

The particle-pair aggregation velocities corresponding to the individual and combined flow fields are presented in Figure 5B. As expected from the streamlines in Figure 4, the EOF (dotted line) is attractive at all separations, and the EHD flow (dashed

(41) Happel, J.; Brenner, H. *Low Reynolds Number Hydrodynamics*; Martinus Nijhoff: The Hague, The Netherlands, 1973.

(42) Solomentsev et al. also included the effect of secondary electrophoresis (i.e., the movement of the charged particle itself in response to the tangential component of the electric field). This contribution is an order of magnitude smaller than the flow forces, however, and is therefore neglected to emphasize the contrasting roles of EOF and EHD flow.

(43) O'Neill, M. E. *Mathematika* **1964**, *11*, 67.

line) is attractive at long separations and repulsive for separations of $r/a < 2.6$. At large separations, EHD flow predominates because the EOF component peaks in magnitude at a closer separation. Notably, the magnitudes of the two flow components are almost equal at $r/a = 3.5$, where Solomentsev et al. began measurements of the particle separation versus time. This suggests that EHD flow contributed significantly to the observed velocities.

The combined flow (solid line) is attractive for all distances $r/a > 2.1$, but according to the theory the repulsive component of EHD flow is greater than the attractive EOF component for distances very close to the particle ($r/a < 2.1$). Experimentally, the particles are always observed to move into close contact (at least as resolvable by optical microscopy), indicating that the theory is incorrect for such close separations. This is to be expected because the calculations for the flow field account for the presence of the second particle only through Faxen's law, which is an approximation. A more detailed analysis that explicitly incorporates the presence of both particles is necessary to resolve the flow field at such close separations.

Nonetheless, an important consequence of the repulsion by EHD flow at intermediate separations ($r/a < 2.6$) is that EHD flow *assists* the dispersal of aggregated particles upon reversal of the field polarity rather than hinders as assumed previously. This behavior is explored in Figure 6A, which shows the streamlines of combined EOF and EHD flow assuming all parameters are identical to those in Figure 5 except that the field polarity is reversed. In practice, this perfect reversal is difficult to achieve as a result of both the transient response of the potential (or current) and the tendency of the particle height to increase in response to the reversed field. Neglecting these complications, however, reveals that the flow structure for reverse polarity has two distinct circulation cells: one that rotates clockwise centered near $z/a = 0.3$ and one that rotates counterclockwise centered near $z/a = 2$. Along the particle centerline, the radial component of the flow is directed outward for $r/a < 3$ and inward for $r/a > 3$.

The calculations of the particle-pair aggregation velocity (Figure 6B) confirm that the flow is strongly repulsive at close separations and weakly attractive for separations of $r/a > 3.4$. This result is consistent with the experimental observations of aggregate breakup upon reversal of polarity, and contrary to expectations, EHD flow contributes significantly to the dispersal.

Indeed, the theory suggests that particles under reverse polarity will form "loose" aggregates with relatively large interparticle separations at $r/a = 3.4$ (surface-to-surface separation of $d \approx 1.4a$). Similar structures are observed in oscillatory fields, where the large separations result from a balance between attractive EHD flow and dipolar repulsion.^{16,19,44} Here the large separation results entirely from hydrodynamic effects. However, aggregates might be difficult to obtain in practice. For example, under galvanostatic conditions polarity reversal immediately flips the sign of the current, but the applied potential (which drives the attractive EHD flow) takes much longer to adjust. During this time, EOF flow actively pushes the particles apart and the electric field lifts the particles upward from the electrode, diminishing the magnitude of both flows. A better test might be to apply a field of reverse polarity to widely dispersed particles and wait to see if they form "loose" aggregates. The time scale for loose aggregation under reverse polarity is much longer because the driving force is weaker, which may explain why previous investigators have not observed it.

Thus far we have focused on the predicted particle-pair velocities, but Solomentsev et al. measured the particle position

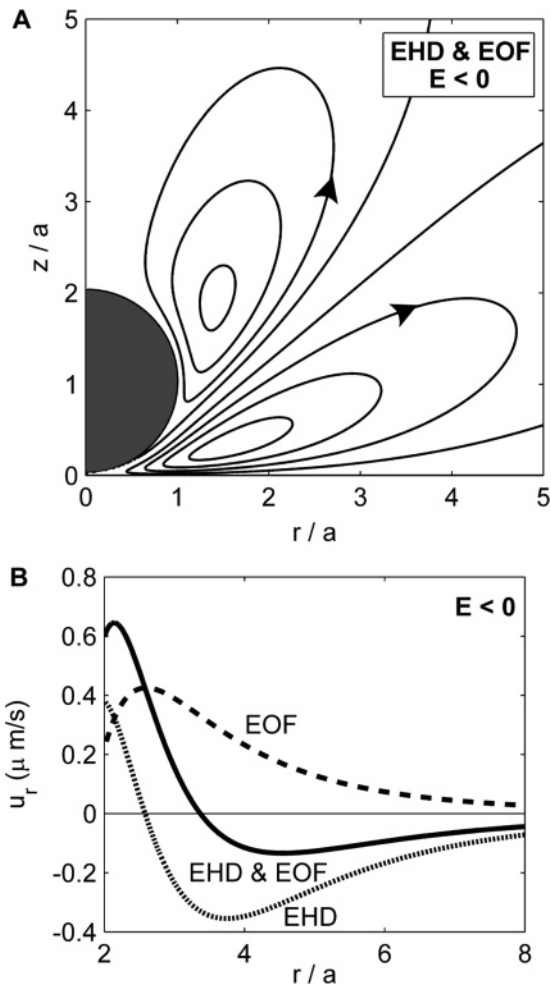


Figure 6. Superposition of EOF and EHD flow for the experimental conditions reported by Solomentsev et al.¹⁴ with reversed polarity. All other parameters are the same as in Figure 5. (A) Streamlines for the superposition of EOF and EHD flow with reversed polarity. Arrows indicate the direction of flow. (B) Radial particle-pair aggregation velocity with reversed polarity. Symbols: (\cdots), EHD velocity; ($- -$), EOF velocity; ($-$), combined EOF and EHD. The combined flow is strongly repulsive at close separations but weakly attractive at larger distances.

versus time rather than the velocity.¹⁴ To test the theory directly against their data, we computed position–time data from the aggregation velocity by means of a first-order explicit forward Euler scheme. Representative results of these computations are presented in Figure 7. The marker symbols represent the position versus time for 10 different particle pairs under ostensibly identical conditions. The differences in slope indicate that each particle pair moved with a significantly different velocity, and Solomentsev et al. confirmed that Brownian motion is insufficient to explain the variability.¹⁴ Several effects could account for the scatter, such as differences in zeta potential, particle size, and height over the electrode, but Solomentsev et al. took pains to minimize these sources of error. Moreover, they found that the amount of scatter increased with the applied field strength. They speculated that EHD flow might be responsible for the variability.

Our calculations confirm that EHD flow could account for the increased scatter, provided that the applied potential was not carefully controlled during each experiment. (Solomentsev et al. did not report the applied potentials.)¹⁴ The three solid curves in Figure 7 are the predicted separation versus time curves for three different values of the applied potential: $\Delta\phi = 0, 0.5,$ and 1.3 V for the top, middle, and bottom curves, respectively. The

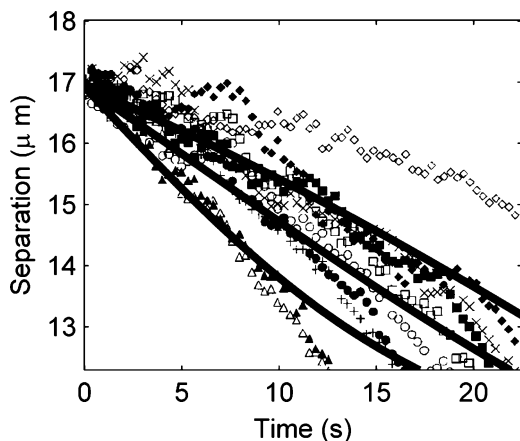


Figure 7. Comparison of the theory with experimental measurements by Solomentsev et al.¹⁴ of particle-pair separation versus time for 9.7- μm -diameter particles ($\zeta = -65$ mV) suspended in 1.0 mM sodium bicarbonate over a gold electrode with a 60 V/m field. Each symbol shape represents 1 particle-pair trajectory; each of the 10 trajectories represents a different pair of nominally identical particles under ostensibly identical conditions. The three solid curves are the theoretical separations based on electrically induced flow. (Top curve) flow due to EOF only. (Middle curve) superposition of EOF and EHD flow induced by an applied potential $\Delta\phi = 0.5$ V. (Bottom curve) superposition of EOF and EHD flow induced by an applied potential of $\Delta\phi = 1.3$ V. The two EHD curves demonstrate that differences in the EHD velocity, due to different degrees of electrode polarization, could account for some observed scatter. Note that both EOF and EHD flow predict deceleration at close separations but acceleration is observed. Experimental data points are reproduced from Figure 8 in reference 14.

top curve represents the position versus time curve resulting solely from EOF, with no EHD contribution. The other two curves represent the combined influence of EOF and EHD flow for different applied potentials. Clearly the EHD flow could account for much of the scatter if the potential varied between experiments. The potential increases continuously after application of a constant current, so the influence of EHD flow could depend on how much time was required for the two particles to reach $r/a = 3.5$. Likewise, organic residues and oxide layers of varying thickness on the electrodes are well-known sources of variability in electrochemistry.²³ The increase in scatter with field strength is consistent with an EHD mechanism because the influence of EHD flow increases with field strength and differences in applied potential are more likely to be manifested.

A final aspect of the predicted particle-pair positions is that the shape of the curve is qualitatively incorrect at very close separations. Specifically, the theory for both EOF and EHD flow predicts that the particles will decelerate as they approach, but the observation is that they accelerate. It is unsurprising that the theory breaks down at very close separations because Faxen's law serves only as an approximation of the hydrodynamic forces on each particle. Particle rotation might also affect the aggregation velocities.⁴⁵ Furthermore, other effects, such as electrophoretic and dielectrophoretic forces, might play non-negligible roles at

close separations. More detailed calculations are necessary to explore the forces at close separations.

Summary and Conclusions

Scaling expressions for the EHD fluid velocity engendered by the dipole field of a polarized particle near an electrode with a faradaic current were derived. According to the analysis, the flow velocity is proportional to the product of the applied potential and faradaic current density, and the direction of flow depends on the sign of the dipole coefficient. Analytical expressions were derived for the electric field and corresponding EHD streamlines around a single polarizable particle near an electrode. Comparison of the EOF and EHD flow indicates that attractive EHD flow predominates far from the particle, whereas attractive EOF predominates over the repulsive EHD flow close to the particle. Moreover, EHD flow can account for the observed scatter in aggregation assuming variability in the applied potential between experiments.

Although these results are consistent with previous experimental observations, more direct experiments are necessary to confirm the significance of EHD flow in steady fields. One test is to look for the formation of loose aggregates under reverse polarity, which would confirm the existence of a long-range attractive force. Alternatively, the scaling analysis suggests a possible experimental approach based on modification of the particle surface charge. Because EOF depends on the particle zeta potential, it should be possible to eliminate EOF by adjusting the electrolyte such that the zeta potential is zero (i.e., the isoelectric point). The dipole coefficient would remain nonzero, however, so EHD flow should be observable without any accompanying EOF. Although using particles at the isoelectric point introduces complications due to particle flocculation, future experimental work may benefit from this approach.

Similarly, the dependence of EHD flow on the dipole coefficient suggests that mixtures of particles with varied dipole coefficients might exhibit diverse morphologies, as observed in oscillatory fields.⁴⁶ Alternatively, kinetic experiments examining the aggregation behavior of large numbers of particles could be compared to numerical simulations of aggregation that incorporate either EOF alone or the superposition of EOF and EHD flow. Any experimental or numerical tests will benefit from more detailed calculations of the fluid streamlines around two adjacent particles to gauge the hydrodynamic forces at close separations more accurately.

Acknowledgment. This work was supported by NASA OBPR, the NASA University Research, Engineering, and Technology Institute on BioInspired Materials (BIMat) under award nos. NCC-1-02037, NSF/DMR-0213706, and ARO/MURI under grant no. W911NF-04-1-0170. Partial support for W.D.R. was provided by NASA GSRP.

LA062870L

(45) Santana-Solano, J.; Wu, D. T.; Marr, D. W. M. *Langmuir* **2006**, *22*, 5932.

(46) Ristenpart, W. D.; Aksay, I. A.; Saville, D. A. *Phys. Rev. Lett.* **2003**, *90*, 128303.